Proceedings of the Korea Nuclear Society Spring Meeting
Cheju, Korea, May 2001

Investigation on Initial Defect Structures in Unirradiated Reactor Pressure Vessel Steels by Positron Lifetime Measurements

Eung-Seon Kim, Se-Hwan Chi and Jun-Hwa Hong
Korea Atomic Energy Research Institute

Yeon-Keun Shim, Keun-Ho Lee
Institute for Advanced Engineering

Abstract

Positron lifetime (PL) measurements on the three kinds of reactor pressure vessel (RPV) steel and one kind of Linde 80 weld were performed at room temperature with a fast coincidence system to investigate initial defect structure and to prepare baseline PL parameters for future comparison with that of irradiated one. Optical microscope (OM) and transmission electron microscope (TEM) was used for microstructural characterization. The RPV steels showed largely the same tempered bainite microstructure, however, noticeable differences were observed in the grain size, distribution of cementite, and bainitic lath width. Variations in positron lifetime among the three kinds of RPV steel of similar chemical composition were definitely observed and were interpreted as the difference in initial defect structures originated from the different manufacturing process. In the case of the Linde 80 weld, the longer lifetime component which did not appear in the RPV steels was discussed in terms of nonmetallic inclusions.

I. Introduction

The irradiation embrittlement of RPV steel by fast neutron has been investigated extensively during the past two decades. A number of semi-empirical models based on macroscopic data have been established but these models have not been validated sufficiently as far as underlying microstructural mechanisms are concerned. The radiation-induced defects are very small objects which are not observed by common metallographic techniques such as optical or transmission electron microscopy with the visibility limit of 5 nm. Hence, some other atom probe methods are needed to resolve and identify the defect structures. Positron annihilation spectroscopy (PAS) has been effectively applied for investigating the micromechanisms of the irradiation embrittlement of RPV steels [1-3]. This is mainly due to the sensitivity and selectivity of PAS to open-volume defects of the size as small as a single vacancy and

nondestructive nature [4]. Radiation-induced vacancy-type defects such as vacancies, vacancy-impurity pairs, dislocations, microvoids, etc., act as attractive positron trapping sites. The lifetime of positrons trapped at theses defects is longer than that of free positrons in the bulk. As a result of the presence of the open-volume defects, the average positron lifetime observed in structural materials would be expected to increase with radiation damage. However, the radiation-induced defects interact with initial defects such as dislocations, precipitates, misfits on the grain boundaries in unirradiated materials, it is necessary to investigate initial defect structure of unirradiated material and to prepare baseline PL parameters for future comparison with that of irradiated microstructure.

In this study, to investigate the initial defect structures in unirradiated RPV steel, we performed PL measurements on one kind of Linde 80 weld and the three kinds of RPV steel of similar chemical composition which differ in microstructures partly due to the difference in manufacturing process. The present work serves as a first step of a research program involving the investigation of the irradiated RPV steels in the future.

II. Experimental Procedures

II-1. Microstructural Investigation

One kind of Linde 80 weld and three kinds of SA508 Cl. 3 RPV steel produced by different manufacturing process, especially steel refining process were used in this investigation. Chemical composition and the employed refining process of the RPV steels are shown in Table 1. Grain sizes were determined by three circle (Abrams) procedure of ASTM E-112 at × 400 on specimens polished to 0.3 μm Al_2O_3 powder, etched in 1.5 ~ 3 % Nital for 10 ~ 20 sec. Microstructures and carbide morphologies, as well as size and numbers, were investigated by TEM (JEOL 2000FX) on thin films and carbon replicas at 1/4 *t* materials, where *t* is the nominal material thickness. Thin films were prepared by submerged, electrolytic jet-thinning technique in a solution of 10 % perchloric acid at 30 to 35 V. Carbon extraction replicas were prepared from surfaces etched with 4 % Nital for 60 – 120 sec., carbon coated in a Veeco high vacuum evaporation chamber, and secondary etched in 10 % HCl + 90 % Ethanol solution at about 0.1 ampare for about 4 – 5 minutes.

II-2. Positron Lifetime Measurement

For PL measurements, square samples of 10 × 10 mm in size were prepared from fractured Charpy-V bodies by cutting. The surfaces were successively ground with SiC paper and carefully polished with diamond paste with grains of 1 μm to remove the surface damage and reduce the sample thickness from 0.5 mm to 0.25 mm. It was reported that no dependence on the sample preparation was observed in comparative measurements [5]. However, to examine the visibility of reducing radiation exposure by

minimizing sample preparation step, we performed auxiliary PL measurements on the as-cut and as-ground to 2400 grit samples (YK5).

The PL measurements were performed at room temperature by means of a fast coincidence system at Institute for Advanced Engineering. The schematic diagram of the system is shown in Fig. 1. The time resolution of the system was 230 ps (FWHM) for 511 – 1274 keV gamma-coincidences. The ^{22}NaCl positron source with an activity of about 10μCi was sealed between 2 μm thick kapton foils and sandwiched between samples. Cylindrical fast plastic scintillators are used for γ-ray detection and each scintillator was optically coupled to a photomultiplier tube. At least 4×10^6 counts in the whole spectrum were collected for each sample. The spectra were analyzed with the PATFIT-88 program after subtracting source correction due to the contribution of positrons being annihilated in the positron source. The source correction and the time resolution of the spectrometer were determined from the lifetime spectrum analyses of annealed Al reference samples (99.999%).

III. Results and Discussion

III-1. Comparison of Microstructure

The results of microstructural investigation by optical microscope and TEM (thin film, carbon replica) on 1/4 *t* materials are summarized in Table 2. Fig. 2 shows typical carbide morphology, size, and distribution taken by TEM (thin film) on 1/4 *t* materials. The three kinds of steel showed largely the same bainitic microstructure prevailing in RPV steels. There were some differences in grain size, especially between YK3 and YK5, JSW. The grain size of YK3 is 50 % larger than the YK5 and almost double that of JSW. The absence of aluminum addition in YK3 versus YK5, JSW can account for the larger grain size [6]. Round cementites and acircular Mo_2C carbides were found in all steels. There was no apparent difference in the size of acircular Mo_2C, but the size of the cementite particle in YK3 was about 10 ~ 20 times larger than that of JSW. Moreover, large agglomerated islands of round cementites were frequently observed in YK3, but not in JSW. The agglomerates in YK3 with the size of above 30 μm in length were larger than the average grain size of YK3 (~22 μm). For YK3 and JSW, with roughly the same number density of carbides, the number of needle-like Mo_2C was a little higher in YK3 than JSW. From the TEM (thin film) results, it was observed that the lath boundary in YK3 was not developed well compared to YK5 and JSW. JSW showed the narrowest lath width (2 μm) and YK3 showed the widest (5 μm). Interlath carbides were found in YK3 and YK5, and were thickest in YK3. A low cooling rate during quenching has been attributed to the growth of interlath carbides [7]. The microstructure of K1W is shown in Fig. 3. The morphology and distribution of carbides were usual one observed in Mn-Mo-Ni alloy welds, however, many nonmetallic inclusions with granular shape were observed. The average size of the inclusions was about 0.8 μm and some inclusions were larger than 2 μm.

III-2. Positron Lifetime

The measured PL spectra were decomposed into three lifetime components after source and foil contributions were subtracted. We neglected the last long-lifetime component of $\tau_3 > 600$ ps with relative the intensity of $I_3 < 1.9$ %. Its present can be explained as the contributions from a surface contamination during handling the samples or a thin surface oxide layer [8]. The measured lifetimes are summarized in Table 3 with the relative intensity I_i and the average positron lifetime ($\tau_m = \Sigma\tau_i \cdot I_i / \Sigma I_i$). The shortest component, τ_1 is commonly interpreted as a result of positron delocalization, probably without any dominant trap [3]. On the other hand, the longer components τ_2 represent contribution of the positrons trapped at defects. All the average positron lifetime observed in this study were significantly higher than the bulk positron lifetime in annealed α-Fe (110 ps), it is thus clearly indicated that a substantial fraction of positrons is trapped at defects in the present steels. The expected defect structure in these steels is very complex and it is difficult to assign the observed trapping signal to a specific kind of defect. Nevertheless, by comparing the measured lifetime with ones found in the literature, we can interpret the major defect types in the steels investigated. Positron lifetimes accepted for simple defect configuration in pure iron and carbides in low alloy steels are summarized in Table 4.

In the RPV steels, the lifetime of trapped positrons, τ_2 (128.4 ~ 139.6 ps) are substantially lower than that of positrons trapped in vacancies in α-Fe (175 ps), so we can rule out the existence of vacancy-like defects. But the average lifetimes, τ_m higher than the bulk positron lifetime in annealed α-Fe (110 ps) indicates the presence of certain lattice defects, which might be dislocations, misfit at the carbide/matrix interface [3]. As shown in Fig. 4, the dependence of measured τ_2 on the grain size and the lath width was apparently observed. According to positron trapping model [11], the longer the observed positron lifetime is, the higher is the positron trap concentration in the sample. Since dislocation is related with grain boundary, so that the dependence of τ_2 on the grain might be attributed to the presence of a higher dislocation density in YK5 and JSW than in YK3. However, the τ_2 of YK5 (139.6 ps) are even well below the lifetime value accepted for dislocations, we can suppose a significant amount of positrons being trapped by carbide (Fe_3C, Mo_2C) or misfit carbide/matrix interface. It might be supposed that beside possible annihilations in the bulk due to the inhomogeneous distributions of dislocation, complicated trapping processes take place, including dislocation, vacancy-like misfit defects at the carbide/matrix interface, but also carbides itself. A substantial amount of annihilation taking place in carbides itself and misfits at carbide/matrix interface would be a natural explanation of the comparatively low positron lifetime values observed in our RPV steels.

In the Linde 80 weld, the lifetime of trapped positrons (195.1 ps) is higher than those of RPV steels and matches the lifetime of positrons trapped at divacancies. It is considered that this long lifetime came from positrons trapped at nonmetallic inclusion/matrix interfaces as shown in Fig. 3. The low intensity I_2 (40 %) compared with those of the RPV steels might be related with the low volume fraction of the inclusions.

It was found in the as-cut and as-ground samples (YK5) that both lifetimes $\tau_1 \approx 90$ ps and $\tau_2 \approx 160$ ps were longer than those of polished YK5. The $\tau_2 \approx 160$ ps can be attributed to positrons trapped at the dislocations introduced into the samples by cutting and grinding. From this result, it is concluded that irradiated sample must be polished in the same manner as the unirradiated samples were prepared to compare each other.

IV. Conclusions

PL measurements were conducted on a kind of Linde 80 weld and three kinds of RPV steel of similar chemical composition but in difference in TEM microstructure due to different manufacturing process. Positron lifetime results can be summarized into the following items:

1. In the RPV steels, positrons may be trapped at the initial defects including dislocation and misfit at carbide (Fe_3C, Mo_2C)/matrix interface. The dependence of the lifetime on grain size may be attributed to the increase in dislocation density with decreasing the grain size.

2. In the Linde 80 weld, the long lifetime τ_2 (195.1 ps) may be attributed to the positrons trapping at nonmetallic inclusion/matrix interfaces. The relatively low intensity I_2 (40 %) compared with those of the RPV steels might be related with low volume fraction of the inclusions.

Reference

[1] G. Brauer, L. Liszkay, B. Molnar, R. Krause, Nucl. Eng. Design 127 (1991) 47.

[2] R. Paeja, N. De Diego, R. M. De Le Cruz, J. Del Rio, Nucl. Technol. 104 (1993) 52.

[3] C. Lopes Gil, A. P. De Lima, N. Ayres De Campos, J. V. Fernandez, G. Kogel, P. Sperr, W. Triftshauser, D. Pachur, J. Nucl. Mater. 161 (1989) 1.

[4] P. Hautojarvi, Positrons in Solids, Springer, Berlin, 1979.

[5] V. Slugen, D. Segers, P. M. A. de Bakker, E. De Grave, V. Magula, T. Van Hoeche, B. Van Waeyenberge, J. Nucl. Mater. 274 (1999) 273

[6] Sterne, R. H., and Steele, L. E., 1969, Nucl. Eng. Design, 10 (1969) 259

[7] Ohtani, S., Okaguchi, S., Fujishiro, Y., and Ohmori, Y., Metall. Trans. A, 21A (1990) 877

[8] F. Becvar, Y. Jiraskova, E. Keilova, J. Kocik, L. Lestak, I. Prochazka, B. Sedlak, M. Sob, Mater. Sci. Forum 105-110 (1992) 901

[9] P. Hautojarvi, L. Pollanen, A. Vehanen and J. Yli-Kauppila, J. Nucl. Mater. 114 (1983) 250

[10] A. Vehanen, P. Hautojarvi, J. Johansson, J. Yli-Kauppila and P. Moser, Phys. Rev. B25 (1982) 762

[11] W. Brandt, Appl. Phys. 5 (1974) 1

Table 1 Chemical composition of the investigated steels

Material	C	Si	Ni	Mn	Cr	Mo	Cu	P	N	Al	SRP*
YK3	0.18	0.08	0.7	1.40	0.15	0.53	0.06	0.005	0.004	<20pp	VCD
YK5	0.21	0.24	0.9	1.36	0.21	0.49	0.03	0.007	N/A	0.022	SA(I)
JSW	0.19	0.20	0.8	1.44	0.15	0.55	0.03	0.006	N/A	0.020	SA(II
K1W	0.077	N/A	0.6	N/A	N/A	N/A	0.21	0.018	N/A	N/A	-

SRP*: Steel Refining Process VCD: Vacuum Carbon Deoxidation, SA(I) and SA(II): Silicon Deoxidation plus Aluminum treatment in two different factories, I and II

Table 2. Grain size, carbide and precipitates morphology, and banite lath structure in YK3, YK5

Material	Grain Size		Precipitates, Carbide, and Bainite Morphology and Lath width (μm)
	ASTM	Size(μm)	
YK3	7.6	22.3	Round(dia: ~0.5μm), Fine needle(50~100nm) Agglomerated, large and localized coarse carbides Underdeveloped lath boundary, lath width: 5μm Coarse interlath carbide PPt No: $6\times10^7/mm^2$(Round:Needle=1:0.85)
YK5	8.7	15.4	Round(dia:0.025μm), Needle(80nm), Square-like needle(100nm), Three types of carbides morphology, PPts at GB and matrix Well developed lath boundary, lath width: 3.5μm Interlath carbides, PPts No.:$3.1\times10^9/mm^2$ Round:Needle:Square Needle=1:1.75:0.46
JSW	9.5	12.5	Round(<0.05μm), Needle(50~100nm), Fine round carbide Well developed lath boundary, lath width:2μm No interlath carbide, PPts No.:$6.7\times10^7/cm^2$, Round:Needle=1:0.39

Table 3. Three-components decomposition of PL spectra of the present steels

Material	χ^2/ν	τ_m (psec)	τ_1 (psec)	τ_2 (psec)	I_1 (%)	I_2 (%)
YK3	1.060	120.2	82.8	128.4	17.6	82.3
YK5	1.067	122.2	65.4	137.1	20.2	79.5
JSW	1.036	128.9	51.6	139.6	12.1	87.5
K1W	1.045	143.5	108.6	195.1	58.4	40.0
Ground	1.177	139.3	90.8	155.5	24.7	74.0
As-cut	1.094	145.5	92.0	161.1	22.1	76.0

Table 4. Positron lifetimes for defect configuration in α-Fe and carbides in low alloy steels [1, 9, 10]

Material	Positron lifetime [ps]
Fe-bulk	110
Fe-edge dislocation	142
Fe-screw dislocation	165
Fe-monovacancy	175
Fe-6V microvoid	304
Fe_3C	101
Mo_2C	112

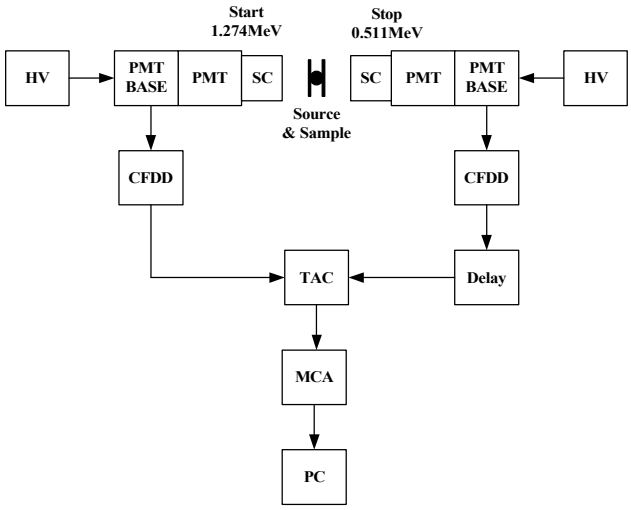

Fig. 1. Schematic diagram of PL measurement system. SC: scintillator, PMT: photomultiplier tube, HV: high voltage power supply, CFDD: constant fraction differential discriminator, TAC: time to amplitude converter, MCA: multi-channel analyzer

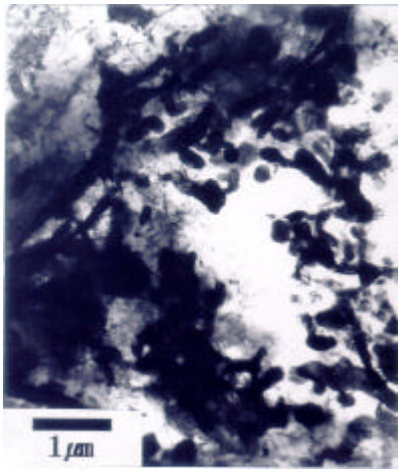

(a) YK3

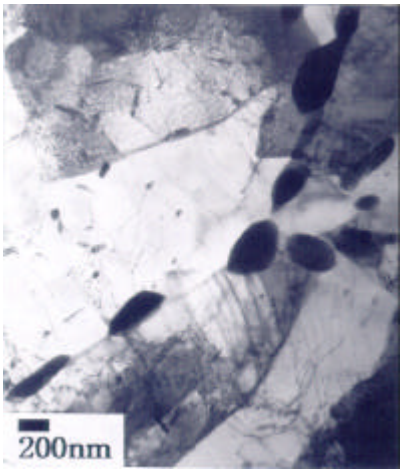

(b) YK5

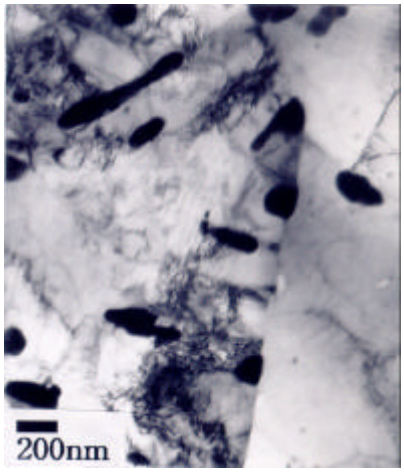

(c) JSW

Fig. 2 TEM (thin film) micrographs of RPV steels YK3, YK5 and JSW

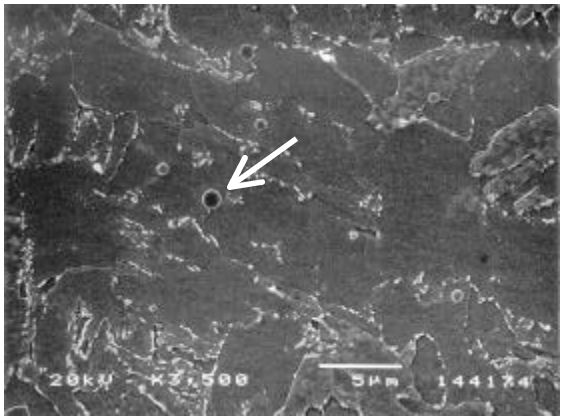

Fig. 3 SEM microstructure of the Linde 80 weld, K1W

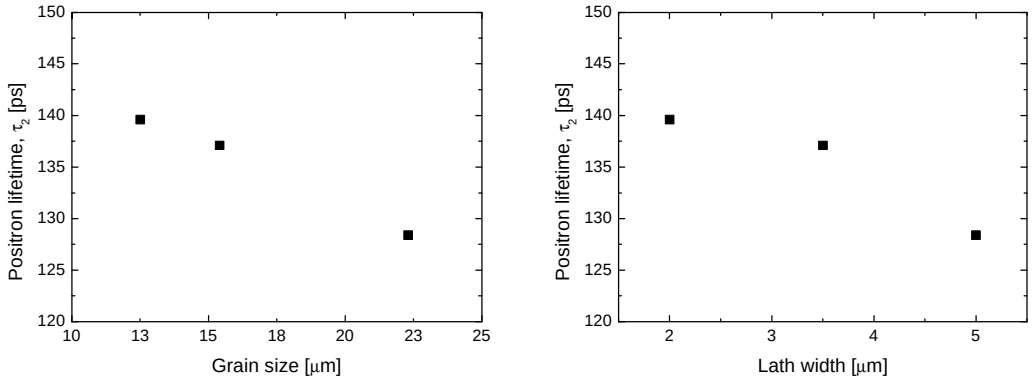

(a) (b)

Fig. 4. Dependence of the positron lifetime, τ_2 on (a) grain size and (b) lath width in the RPV steels